Distributed-Parameter Large Basin Runoff Model. II: Application

Thomas E. Croley II[1]; Chansheng He[2]; and Deborah H. Lee[3]

Abstract: Following the derivation of a distributed-parameter large basin runoff model from a lumped-parameter version for the Great Lakes in the companion paper, we here apply it to the Kalamazoo River watershed in southwest Michigan. First we review relevant similar efforts and then describe the digitization of the watershed into a network of cells through which watershed internal flows are routed. We present the technology used on the Kalamazoo River to create grids of topography, soils, land use, and vegetation data. We describe the calibration of both lumped-parameter and distributed-parameter runoff models on the Kalamazoo River and use observed spatial data variations in our parameter determinations. We investigate alternative evapotranspiration schemes, spatial parameter patterns, solar insolation interpretations, and temporal scaling and compare model results. We suggest model extensions for future work.

DOI: 10.1061/(ASCE)1084-0699(2005)10:3(182)

CE Database subject headings: Parameters; River basins; Runoff; Michigan; Hydrologic models.

Background

The development of large-scale operational hydrologic models is essential for support of long-term water resource planning and management over large river basins. Large-scale operational hydrologic models are defined over large areas ($>10^3$ km^2) and long timescales typically for use over monthly and annual or longer timescales at a daily interval. Large-scale models are often constrained by limited data availability, computational requirements, and model application costs over larger areas, so they must have few parameters, use easily accessible meteorological and hydrologic databases, and be user-friendly. Because of such limits, many large-scale hydrologic models—including the Stanford Watershed Model (Crawford and Linsley 1966), the United States Geological Survey's Precipitation-Runoff Modeling System (Leavesley and Stannard 1995), the Hydrologic Simulation Program in *FORTRAN* (Bicknell et al. 1996), and the Large Basin Runoff Model (Croley 2002)—are spatially lumped parameter models and hence do not adequately take into account the effects of spatial variations of landscape.

The Large Basin Runoff Model (LBRM) of the Great Lakes Environmental Research Laboratory (GLERL) is a lumped-parameter, interdependent tank-cascade model (Croley 2002). It uses mass continuity equations coupled with linear reservoir concepts, and it consists of four components: land surface, upper soil zone, lower soil zone, and groundwater zone. The LBRM uses readily available daily climatological and hydrologic data, requires few parameters and data, and is applicable to other large watersheds beyond the Great Lakes basin. However, spatial variability of watersheds is not fully incorporated in the lumped-parameter LBRM. With the rapid development in computing technology and the increasing availability of multiple digital databases, a distributed LBRM is possible to utilize available databases and new algorithms in simulating rainfall-runoff in large basins. The companion paper by Croley and He (2005) discusses differences between micro- and macroscale models and proposes a framework to modify the macroscale lumped-parameter LBRM to a 2D distributed LBRM. In this paper, we present the implementation results of the 2D LBRM framework to the Kalamazoo River basin in southwest Michigan; Fig. 1. We first describe processing multiple databases and calibrating the 2D LBRM, then present model application results to the study watershed, and finally discuss alternative model structures for future development and refinement.

Discretizing Watershed

Spatial variations of precipitation, soil, vegetation, and topography have significant impacts on runoff modeling (Beven 2000). Although lumped-parameter models treat the catchment as a single unit, with state variables representing averages over the entire catchment area, distributed models make predictions that are distributed in space, with state variables representing local averages. These local averages are defined over a number of elements or grid squares and are obtained by solving the equations for the state variables associated with every element (Beven 2000). Compared with lumped models, distributed models (even simple 2D ones) take into account the variation of spatial heterogeneity and help modelers and resource planners better understand the spatial response to hydrologic events; e.g., see the areal, nonpoint source watershed environment response simulation (ANSWERS) model (Beasley et al. 1980) and the variable infiltration capacity model (Liang et al. 1994). Available topographic

[1]Research Hydrologist, Great Lakes Environmental Research Laboratory, 2205 Commonwealth Blvd., Ann Arbor, MI 48105-2945.

[2]Associate Professor, Dept. of Geography, Western Michigan Univ., 3234 Wood Hall, Kalamazoo, MI 49008-5424.

[3]Hydraulic Engineer, Water Management Team, U.S. Army Engineer Division, Great Lakes and Ohio River Corps of Engineers, P.O. Box 1159, Cincinnati, OH 45201-1159.

Note. Discussion open until October 1, 2005. Separate discussions must be submitted for individual papers. To extend the closing date by one month, a written request must be filed with the ASCE Managing Editor. The manuscript for this paper was submitted for review and possible publication on July 7, 2003; approved on September 7, 2004. This paper is part of the ***Journal of Hydrologic Engineering***, Vol. 10, No. 3, May 1, 2005. ©ASCE, ISSN 1084-0699/2005/3-182–191/$25.00.

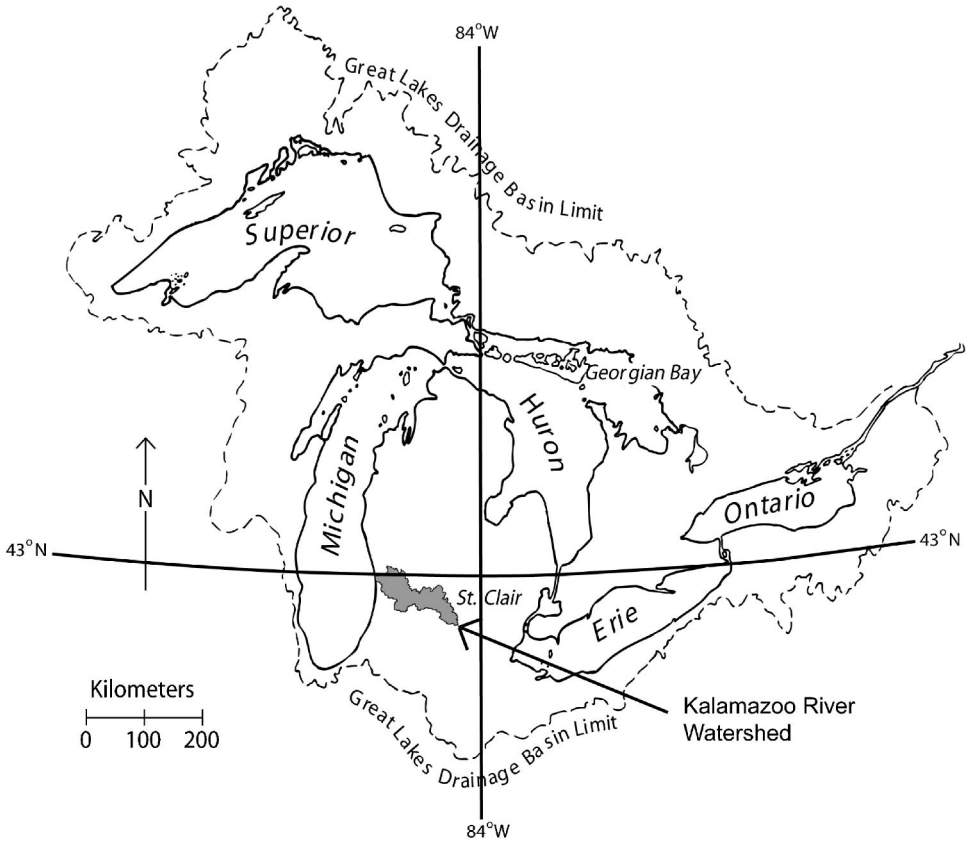

Fig. 1. Great Lakes location map

databases and algorithms make the development of distributed models readily feasible. Operational models should take advantage of available databases for elevation, hydrography, soils, and meteorology to account for spatial variations of climate, soil, topography, vegetation, and land-use practices. Watersheds should be discretized into either grids or hydrological response units; large-scale operational models then should be applied to each resulting cell, and the output from each cell should be routed to the watershed outlet.

Although discretization of watersheds has been a very important topic in recent years, research is still evolving. Wood and Lakshmi (1993) proposed the use of a representative elementary area (REA) for representation of spatial variability. The REA, ranging in size from 1–2.25 km^2 to 5–10 km^2, is defined as the fundamental scale for detailed spatial modeling of hydrological processes. Beyond the REA, a statistical approach can be used to model the hydrological processes to simplify the computational burden. Goodrich et al. (1997) propose the concept of "a critical transition threshold area" of about 37–60 ha (0.37–0.6 km^2) and report that watershed runoff response becomes more nonlinear with increasing watershed scale beyond that threshold area. Other researchers have proposed the concepts of hydrologically similar units (HSUs) and hydrologic response units (HRUs) to represent aggregate areas of similar hydrologic behavior on the basis of topography, land use, soil, and vegetation (Becker and Braun 1999; Karvonen et al. 1999). This approach, as compared with the grid approach (systematically discretizing the watershed into a grid of squares), is more efficient computationally as a specific set of model parameters and is applicable to each type of HRU or HSU. For 2D hydrologic modeling at large scales, discretization of the study watershed into either grids or HRUs appears to be a feasible way to represent the spatial variability of the watershed. The size of the grids or HRUs should be determined by comprehensive consideration of the characteristics of climate, topography, soil, land use, and vegetation in the study area.

Present Technology

In this study, the current lumped-parameter LBRM is expanded to two (spatial) dimensions for a study watershed represented in a grid system (Croley and He 2005). Since determining HRUs involves the integration of soil, vegetation, and topography information and since there are no standard procedures to define HRUs and relevant input parameters for each HRU, we chose to discretize the study watershed into a grid of 1 km by 1 km cells (to match existing areal coverage of meteorological data) based on the watershed boundary determined by using a GIS interface, the ArcView Nonpoint Source Modeling (AVNPSM) interface by He et al. (2001). Subsequently, model parameters are defined for each grid cell on the basis of soil, topography, and vegetation. The modified 2D LBRM is then applied to each 1 km^2 grid cell, and the output flow from each cell is routed accumulatively downstream.

A digital elevation model from the U.S. Geological Survey (at 1:250,000 scale) is used to derive topographically related parameters (flow direction, receiving cell number, and slope) by the AVNPSM. Fig. 2 shows elevation and slope for the Kalamazoo River watershed. Flow from a cell can flow into one of eight adjacent cells downstream on the basis of the slope differences among them. Subsequently, each grid is assigned a flow direction and a receiving cell number (a cell that receives the flow from the adjacent upstream cell). As the flow net allows only one outlet,

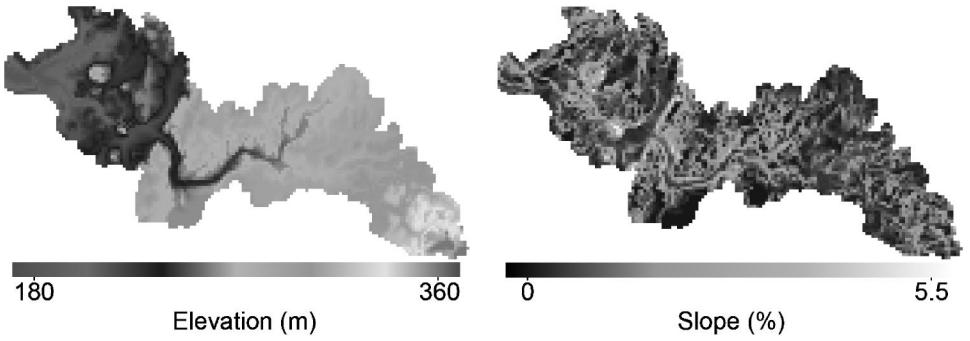

Fig. 2. Kalamazoo River watershed elevation and slope (1 km^2 resolution)

flow directions must be carefully inspected to eliminate any flow loops (Croley and He 2005). A utility module in the AVNPSM was used to check such errors and allow a user to edit flow direction either by one cell at a time or several cells at a time (He et al. 2001). The verified flow net is then used to route flow (Croley and He 2005). A 1:250,000-scale USGS 1990 land-cover database (USGS Prototype 1990 Conterminous U.S. Land Cover Characteristics Data Set CD-ROM) is used to derive a land-cover category (code) for each grid cell by the AVNPSM; see Fig. 3. By using the suggested values in Table 1 to associate flow roughness to land cover (Mays 2001; Dingman 2002), Fig. 3 also shows flow roughness as Manning's *n*.

A state soil geographic database (STATSGO) is used to derive depth, available water capacity (AWC), soil texture, and permeability for upper and lower soil zones. Although some research (Cosby et al. 1984; Abdulla et al. 1996; Yu et al. 2001) has estimated hydraulic conductivity from soil texture and porosity, it is listed as permeability in STATSGO. STATSGO Soil Layer 1 is used as the upper soil zone (USZ) for the LBRM, and Layers 2 to 6 are used as the lower soil zone (LSZ). Values of depth and AWC for Layers 2 to 6 are aggregated to generate area-weighted values for the lower soil zone. First averaging the low and high values of permeability for each of Layers 2 through 6 and then weighting by the relative depth of each layer determine the average permeability for the lower soil zone. Average depth, AWC, and permeability in the USZ and LSZ are further weighted areally to determine their value for each soil association (soil association is a unit on which soil information is mapped and assembled) (USDA SCS 1993). The derived soil depth, AWC, texture, and permeability by map unit are then assigned to each grid cell by the AVNPSM interface (He et al. 2001). Fig. 4 shows upper and lower soil-zone depth and permeability.

Calibration

Lumped-Parameter Large Basin Runoff Model

Calibration began with the lumped-parameter LBRM applied to the Kalamazoo River basin (one "cell" defined for the whole 5,612-km^2 watershed). Calibration consists of a systematic search of the parameter space to minimize the root-mean-square error between actual daily outflow volumes and model outflow volumes. The search consists of minimizing this error for each parameter, selected in rotation, until convergence in all parameters to two or three significant figures is achieved (Croley 2002). This procedure is implemented in *FORTRAN* 95 for IBM-compatible personal computers, suitable for use under either MSDOS or Windows (95, 98, NT, 2000, or XP). The software can also be used to maximize sample correlation between actual and model daily flow volumes. Although this software does not give unique calibrated parameter sets, the hydrology that results from the parameter sets of different calibrations, starting from different initial sets of parameter values, is repeatable. Various calibration periods were tested, as summarized in Table 2. The idea is to use the early part of the 1948–1999 data period for calibration, saving the latter part for later verification studies. The first 2 years of the period are used for model initialization and should not contribute to optimization statistics. Leaving out the first 2 years from the calibration is illustrated in Table 2. We compare the 1948–1957 and 1950–1959 rows or the 1948–1967 and 1950–1969 rows. In both cases, correlation (Column 2) and root-mean-square error (RMSE, Column 3) associated with optimum parameter sets improve. Also, average model outflow is closer to actual (see Column 4). Internal model flow averages (in Columns 5–9) are affected. In Table 2, the 1950–1959 data set yields better statistics

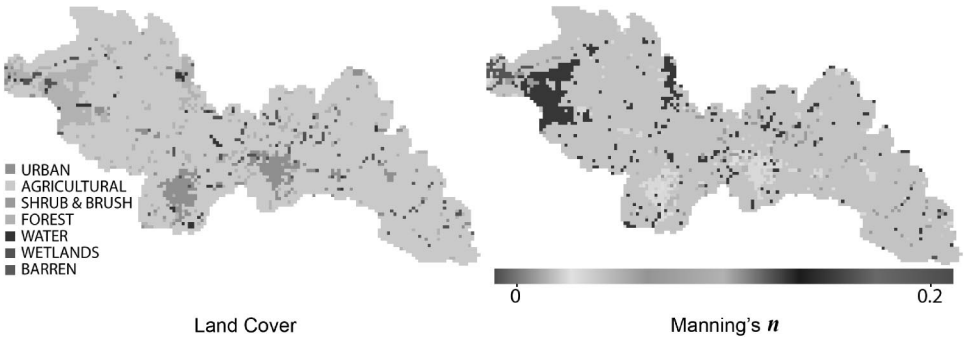

Fig. 3. Kalamazoo River watershed land cover and flow roughness (1 km^2 resolution)

Table 1. Manning's Flow Roughness as Function of Land Cover

Land cover	Manning's n
Urban	0.01
Agriculture	0.04
Deciduous forest	0.24
Evergreen forest	0.41
Water	0.04
Wetland	0.07
Barren land	0.05

than the 1950–1969 set. We wanted to find the data set yielding the best possible fit to minimize parameter determination issues associated with data inappropriateness and allow concentration on model structure in subsequent calibration experiments. Trial and error showed that the 1950–1963 and 1950–1964 periods give the overall best calibrations; the former gives the best correlation, and the latter gives the best RMSE.

Distributed-Parameter Large Basin Runoff Model

We began distributed-parameter LBRM determinations experimentally, keeping each parameter spatially constant over the watershed and changing them one at a time. We compared model outflows with observed values to devise, by inspection, an acceptable starting parameter set for a calibration. Basically, we had to increase the upper soil-zone capacity by an order of magnitude, which controls surface runoff and infiltration; see Eq. (1) in Croley and He (2005). The partial-area concept that the model uses is a large-area concept and is not appropriate for small cell areas at the same value for upper soil-zone capacity. Original values did not allow enough infiltration, resulting in a very "flashy" surface response to all storms. Fig. 5 illustrates with results from the first and last parameter experiments.

We then modified the lumped-parameter calibration procedure for use in a distributed-parameter setting to optimize the spatial-average values of all parameters while imposing a spatial structure onto each parameter over the cells of the watershed. We initially used a shorter calibration period than used for the lumped-parameter calibrations shown in Table 2 to reduce the extensive computation times associated with the distributed model calibration. First, we used no spatial structure in the parameters; i.e., each parameter was taken as spatially uniform over the cells of the watershed. We used the results from the last parameter experiments, just described, as starting values for the parameter calibrations. After calibrating the values of spatially constant parameters, we introduced 10% spatial variation into each parameter, α, according to observed normalized variation in selected data, x

$$\alpha_i = \overline{\alpha}\left[\left(\frac{x_i}{\frac{1}{n}\sum_{j=1}^{n} x_j} - 1\right)\frac{10\%}{100\,\%} + 1\right] - \overline{\alpha}\, f(x_i, 10\%) \tag{1}$$

where α_i=model parameter for cell i; $\overline{\alpha}$=spatial average value for the parameter, determined in a calibration along with values of the spatial average values of the other parameters; x_i=data value for cell i; n=number of cells in the watershed; and

$$f(x_i, \varepsilon) = \left(\frac{x_i}{\frac{1}{n}\sum_{j=1}^{n} x_j} - 1\right)\frac{\varepsilon}{100\%} + 1 \tag{2}$$

For example, the linear reservoir coefficient for basin outflow on cell i, $(\alpha_s)_i$, was taken as ε=10% proportional to the normalized square root of the slope of a cell, as follows:

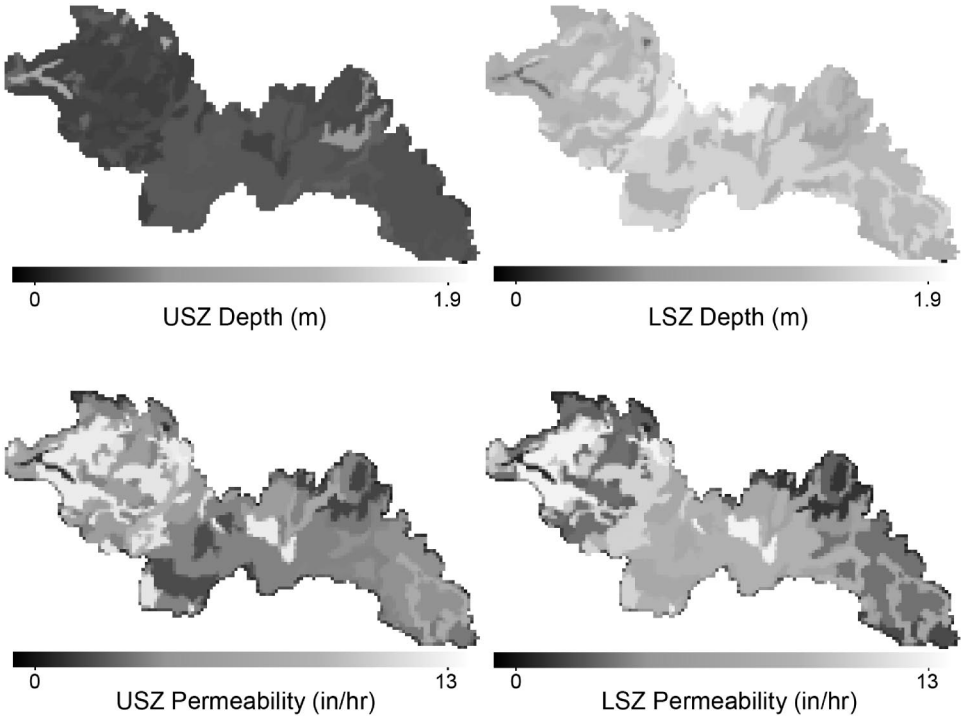

Fig. 4. Kalamazoo River watershed soil-zone depths and permeabilities (1 km^2 resolution)

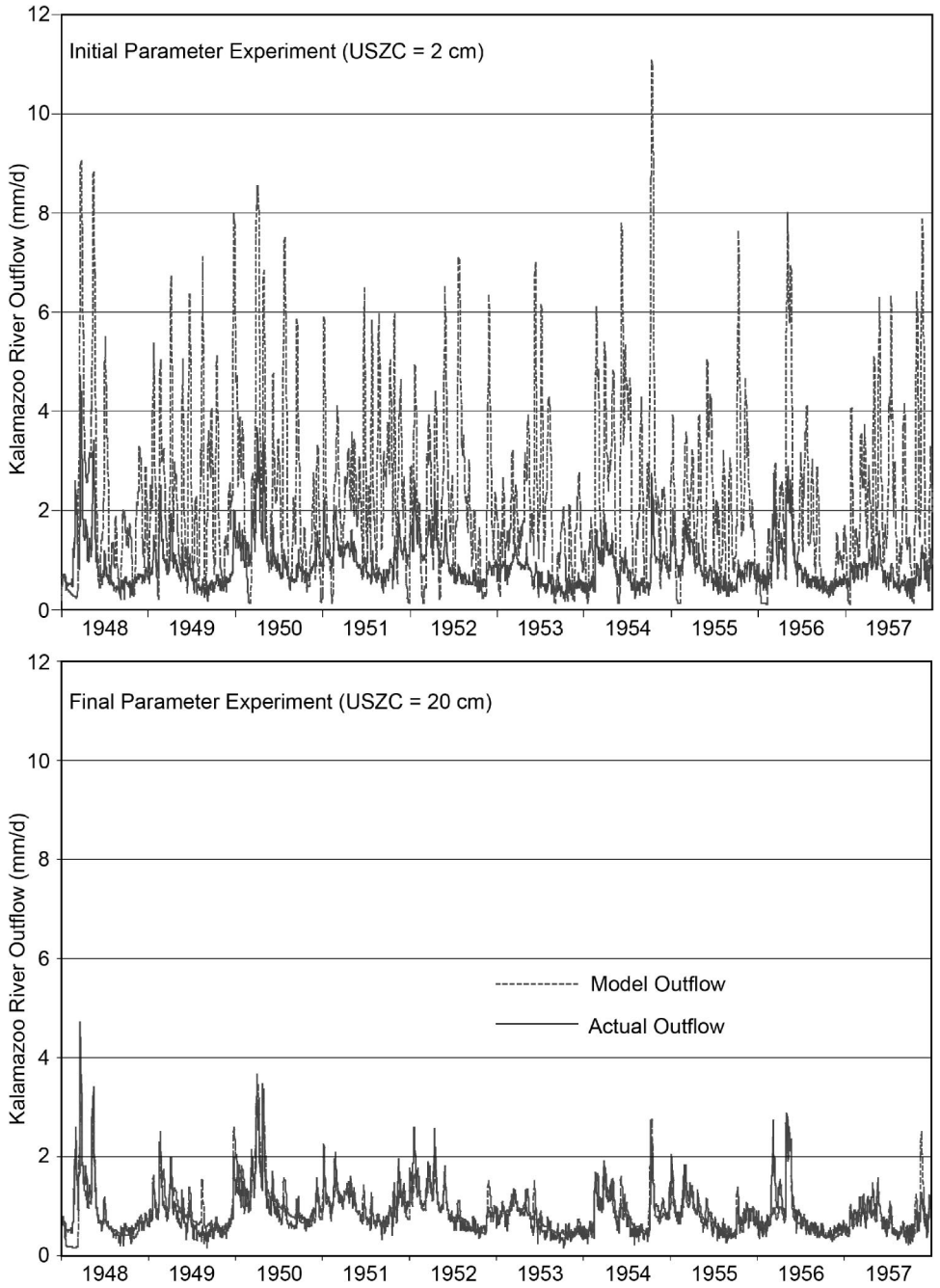

Fig. 5. Distributed-large basin runoff model parameter experiments

Table 2. Selected Summary Statistics for Lumped-Parameter Large Basin Runoff Model Kalamazoo River Calibration

			Long-term average ratio to surface supply					
Calibration period	Correlation	RMSE (cm)	Model outflow	Surface runoff	Interflow	Groundwater flow	Upper zone evaporation	Lower zone evaporation
1948–1957	0.880	0.0224	0.991	0.070	0.050	0.247	0.616	0.008
1948–1967	0.864	0.0217	0.994	0.070	0.039	0.231	0.634	0.017
1950–1959	0.894	0.0190	1.004	0.075	0.036	0.244	0.627	0.005
1950–1969	0.871	0.0202	1.002	0.083	0.019	0.239	0.619	0.030
1950–1964	0.895	0.0184	1.005	0.068	0.032	0.246	0.574	0.074
1950–1963	0.896	0.0185	1.005	0.066	0.035	0.253	0.586	0.056

Table 3. Distributed-Parameter Large Basin Runoff Model Kalamazoo River Calibration Statistics

								Long-term average ratio to surface supply				
V[a]	E[b]	Set[c]	SI[d]	Date[e]	RMSE (cm)	μ_M/μ_A	σ_M^2/σ_M^2	Surface runoff	Interflow	Groundwater flow	Upper zone evaporation	Lower zone evaporation
0	C	—	1	1957	0.0266	0.987	0.946	0.094	0.027	0.258	0.608	0.000
10	C	1	1	1957	0.0261	0.975	0.924	0.084	0.095	0.195	0.598	0.012
20	C	1	1	1957	0.0261	0.976	0.927	0.085	0.089	0.200	0.593	0.016
40	C	1	1	1957	0.0260	0.976	0.930	0.086	0.087	0.202	0.591	0.017
80	C	1	1	1957	0.0259	0.977	0.935	0.083	0.071	0.221	0.583	0.023
80	I	1	1	1957	0.0257	0.981	0.887	0.078	0.087	0.211	0.604	0.010
80	I	2	1	1957	0.0257	0.983	0.898	0.080	0.089	0.208	0.611	0.001
80	I	2	2	1957	0.0258	0.983	0.912	0.085	0.091	0.201	0.610	0.004
80	I	2	3	1957	0.0331	0.978	0.793	0.086	0.289	0.001	0.340	0.274
80	I	2	1	1964	0.0217	1.004	0.829	0.061	0.072	0.222	0.578	0.072

[a]Normalized spatial variation allowed.

[b]Evapotranspiration assumed "complementary to" (C) or "independent of" (I) the potential.

[c]Spatial variation Set 1, given by Eqs. (3)–(7) or Set 2, given by Eqs. (8)–(12).

[d]Solar insolation consideration 1 (use climatic indices for solar insolation and compute heat constant from long-term heat balance); 2 (compute solar insolation from relations used in WGEN, Richardson and Wright 1984); and 3 (use solar insolation based on WGEN directly, no heat constant).

[e]Calibration period end date.

$$(\alpha_s)_i = \overline{\alpha_s} f(\sqrt{s_i}, \varepsilon) \tag{3}$$

where $\overline{\alpha_s}$=spatial average linear reservoir coefficient for basin outflow from a cell; and s_i= surface slope of cell i. Likewise, percolation, interflow, deep percolation, and groundwater-flow linear reservoir coefficients were taken, respectively, as

$$(\alpha_p)_i = \overline{\alpha_p} f\left(\frac{K_i^U}{d_i^U}, \varepsilon\right) \tag{4}$$

$$(\alpha_i)_i = \overline{\alpha_i} f\left(\frac{K_i^U}{d_i^U}, \varepsilon\right) \tag{5}$$

$$(\alpha_d)_i = \overline{\alpha_d} f\left(\frac{K_i^L}{d_i^L}, \varepsilon\right) \tag{6}$$

$$(\alpha_g)_i = \overline{\alpha_g} f\left(\frac{K_i^L}{d_i^L}, \varepsilon\right) \tag{7}$$

where K_i^U=upper and K_i^L=lower soil-zone permeability in cell i; d_i^U=upper and d_i^L=lower soil-zone depth; and $\overline{\alpha_p}$, $\overline{\alpha_i}$, $\overline{\alpha_d}$, and $\overline{\alpha_g}$=spatial average coefficients for percolation, interflow, deep percolation, and groundwater, respectively. Fig. 4 is used to determine the soil-zone depths and permeabilities for Eqs. (4)–(7). After introducing ε=10% spatial variation into each of the preceding parameters, we calibrated to find the best values of the spatial averages. We repeated these calibrations for ε=20, 40, and 80% successive spatial variations to enable the use of calibrated spatial average parameter values from one calibration as reasonable starting values in the next. These calibrations are shown as the first five rows in Table 3. Exploration of more than ε=80% spatial variation in parameter fields indicated that calibrations did not improve; we avoided problems of having zero values for model parameters that would exist at ε=100%.

The first calibration in Table 3 (with no spatial variation in the model parameters allowed) resulted in an error of about 0.27 mm in daily flows but gave near unity values for the ratios of model to actual flow means and variances. Considering 10% spatial variations in the parameters with Eqs. (3)–(7) (second calibration in Table 3) reduced the error but also pulled the ratios of model to actual flow means and variances further from unity. As successively more spatial variation was allowed in the parameters (Calibrations 3–5 in Table 3), all three measures improve; error drops and the ratios of model to actual flow means and variances again approach unity.

Evapotranspiration

The first five calibrations in Table 3 were performed with a distributed LBRM that used complementary evapotranspiration and potential evapotranspiration; see Croley and He (2005). In this case, both potential and actual evapotranspiration depend on the available water supply and sum to equal the heat available for evapotranspiration. If the water supply is large, the daily actual evapotranspiration volume approaches the limit of the water supply or the heat available, and the daily potential evapotranspiration volume approaches zero. If the water supply is small, the daily actual evapotranspiration volume approaches zero and the daily potential evapotranspiration volume approaches the heat available; see Eqs. (14)–(17) in Croley and He (2005).

As discussed by Croley and He (2005), actual and potential evapotranspiration cannot be regarded as complementary when the LBRM is applied to a small cell; they must be replaced with concepts that make sense for the small scale. A more traditional independent concept—that actual evapotranspiration does not affect potential evapotranspiration—is much more appropriate for small areas, such as each of the cells used in the distributed-parameter LBRM application; see Eq. (21) in Croley and He (2005). The distributed-parameter LBRM was recalibrated, starting with the parameter set from the fifth calibration in Table 3, for the case of independent evapotranspiration and potential evapotranspiration. It is listed as Calibration 6 in Table 3.

Considering the changed evapotranspiration mechanics in the sixth calibration in Table 3 gave mixed statistics. The error was reduced, compared with the fifth calibration in Table 3, and the ratio of model to actual flow means improved (closer to unity). However, the ratio of model to actual flow variances was much poorer, suggesting that model output is less variable than actual.

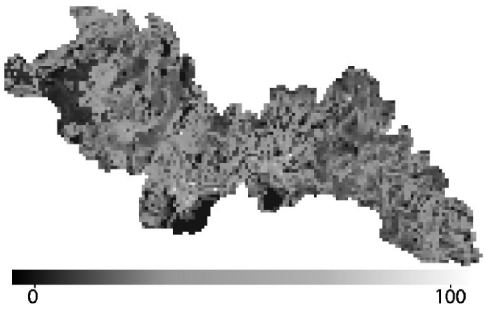

Fig. 6. Kalamazoo River watershed $\sqrt{s_i}/\eta$ (1 km^2 resolution)

Alternative Parameter Spatial Patterns

We also found calibration statistics to improve with this set of spatial variation patterns

$$(\alpha_s)_i = \overline{\alpha_s} f\left(\frac{\sqrt{s_i}}{\eta}, \varepsilon\right) \tag{8}$$

$$(\alpha_p)_i = \overline{\alpha_p} f(K_i^U, \varepsilon) \tag{9}$$

$$(\alpha_i)_i = \overline{\alpha_i} f(K_i^U, \varepsilon) \tag{10}$$

$$(\alpha_d)_i = \overline{\alpha_d} f(K_i^L, \varepsilon) \tag{11}$$

$$(\alpha_g)_i = \overline{\alpha_g} f(K_i^L, \varepsilon) \tag{12}$$

where η=Manning's roughness coefficient. Fig. 6 shows the spatial variation of $\sqrt{s_i}/\eta$, constructed from Figs. 2 and 3. Distributed-parameter calibration statistics for these calibrations, with parameter spatial patterns of Eqs. (8)–(12), are also summarized in Table 3 as Calibration 7. Here we observe that although error remains essentially unchanged—that is, the improvement is too small to be seen with three significant figures, both ratios of model to actual flow means and variances improve compared with the previous calibration in Line 6 which used the same independent actual and potential evapotranspiration mechanics but used the parameter spatial pattern of Eqs. (3)–(7). Furthermore, we observe that with this model calibration, about 61% of the surface supply evaporates, almost entirely from the upper soil zone, and about 21% flows as groundwater.

Insolation

Next, we experimented with alternative solar insolation interpretations. The lumped-parameter LBRM (Table 2) and the distributed-parameter LBRM (Table 3, the first seven calibrations) all use daily solar insolation derived from climatic indices; [see Eq. (20) of Croley and He (2005)], and compute a heat constant, which is based on a long-term heat balance, to use in estimating daily solar insolation from air temperature. We first replaced the calculation of daily solar insolation from climatic indices, used in the computation of the heat constant, with its reverse-engineered calculation (Croley and He 2005) from a weather generator (WGEN) described by Richardson and Wright (1984). We compute daily solar insolation as a function of location, time of year, minimum and maximum air temperature and precipitation for the current and previous day, and previous day insolation. The results are summarized as Calibration 8 in Table 3. It is very similar to Calibration 7; the only difference in the two models is that the insolation, used in computing the heat constant, is computed differently. It gives slightly higher error but has model variation closer to actual than does the previous model. Either is probably suitable for future use.

We next used the reverse-engineered WGEN-derived solar insolation directly, replacing use of the heat constant applied to daily air temperature. Doing so eliminates the need to compute a heat constant in the first place. Results are summarized as Calibration 9 in Table 3. Calibration 9 is much worse in error and variance than model Calibrations 7 or 8. It shifts evapotranspiration from solely the upper soil zone to roughly split between the upper and lower soil zones.

Model Comparisons

The best calibration (that is, Calibration 7 in Table 3) was repeated for the 1950–1964 calibration period so that we could directly compare it with the lumped-parameter LBRM calibration in Table 2; it is shown as the tenth, that is, the last, calibration in Table 3. Although the error is actually higher with the distributed model, both models show very similar ratios of model to actual flow means and very similar long-term average ratios to surface supply of surface runoff, interflow, groundwater flow, upper soil-zone evapotranspiration, and lower soil-zone evapotranspiration. Actually, the RMSE in Tables 2 and 3 only reveals part of the comparison. A better model comparison is given in Fig. 7, which shows the same typical 2-year hydrograph from some of the models. The lumped-parameter model, shown in Fig. 7(a), has very smooth recessions, whereas the distributed-parameter model simulations show more variability in the recessions, as would be expected when spatial variability of rainfall, as well as of parameters, is considered. The difference in recession variability between Figs. 7(a and b) reflects precipitation variability only, since spatial parameters variability is absent in both. Fig. 7(b) shows a little closer match between model and actual flows than does Fig. 7(a), but the biggest improvement occurs between Figs. 7(b and c). The latter allows spatial variability in the model parameters. Likewise, additional improvement occurs between Figs. 7(c and d), representing a change in spatial parameters variation from Eqs. (3)–(7) to Eqs. (8)–(12), respectively.

Temporal Scaling

As illustrated in Tables 2 and 3 and mentioned previously, the goodness-of-fit of the lumped-parameter LBRM, in terms of RMSE, is better than that of the distributed-parameter LBRM. This result is in part attributable to the use of the same internal computation interval (1 day) in both models, since input meteorology for both models is available only at the daily time interval. Presumably, the use of good hourly data would enable the distributed-parameter model to do better. We did explore calibrations using the hourly time interval in the distributed-parameter LBRM but only with daily data values for each of the 24 h in the day. Of course, the computation requirements increased dramatically; however, no better results were obtained with the daily interval. Also, the results were similar between the hourly and daily models, possibly indicating that the daily time interval is small enough to allow the assumptions of constant precipitation, potential evapotranspiration, and upstream surface flow during each time interval (Croley and He 2005). Again, this result is expected to change with the availability of good hourly data and model modifications that recognize diurnal cycles in several processes.

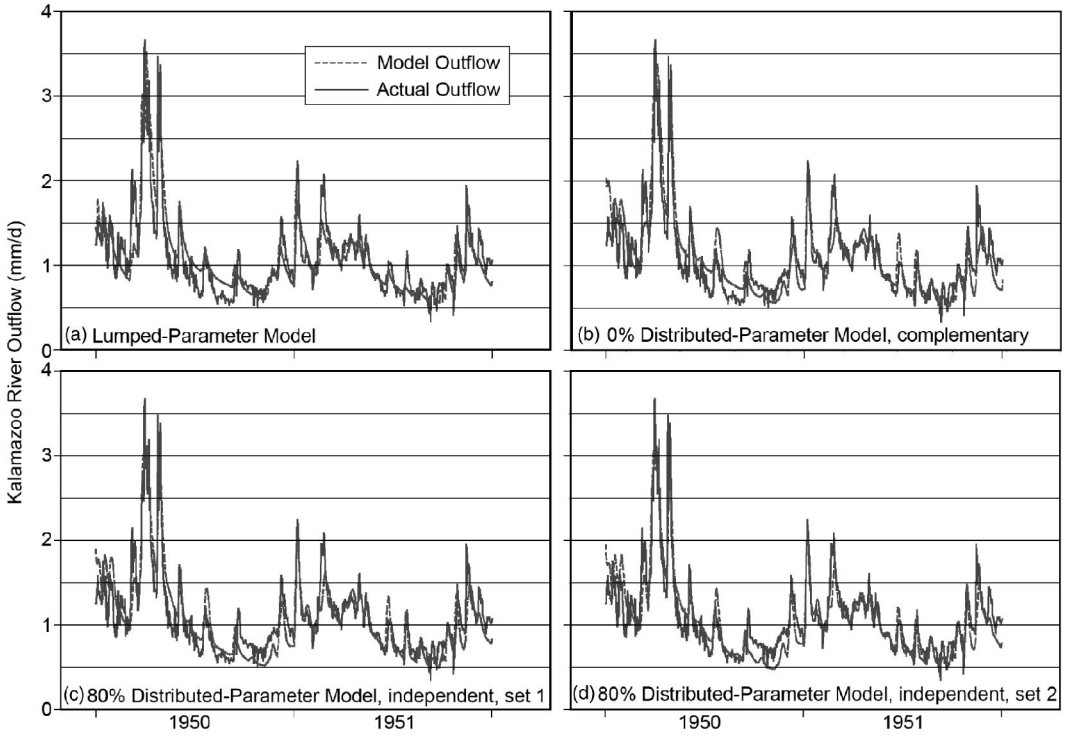

Fig. 7. Selected 1950–1951 model comparisons with actual Kalamazoo River outflows

Extensions

We will explore alternative spatial variation schemes, as in Eqs. (3)–(7) or Eqs. (8)–(12), by utilizing other observable watershed characteristics to relate to spatial parameter variation. We also will explore several model formulation alternatives to improve performance.

Evapotranspiration and Insolation

Since the consideration of evapotranspiration and potential evapotranspiration as independent (appropriate for small scales) improves model performance compared with considering them complementary (appropriate for large scales), we will also explore the more traditional Penman-Monteith (PM) method. The PM method is recommended for estimating daily and longer-period evapotranspiration over a wide range of climate conditions (Jensen et al. 1990; Xu and Singh 1998). It links vegetation effects to evapotranspiration through aerodynamic and canopy resistance terms where detailed databases are available. It appears that necessary data are available at the microscale for several Great Lakes riverine watersheds, including the Kalamazoo and Maumee rivers.

Since the PM method requires aerodynamic and canopy resistance coefficients, databases of vegetation indices from the USGS can be used to infer roughness length (Liang et al. 1994) and to derive canopy resistance (Jensen et al. 1990; Liang et al. 1994; Caselles et al. 1998). Wind-speed data from climatological databases can be converted to 2-m height wind speed by empirical formula (Jensen et al. 1990). Vapor pressure deficit can be computed from minimum and maximum daily air temperatures and dew point temperatures. Net solar radiation can be estimated as previously, with vegetation indices used for estimating emissivity, and soil heat flux generated as a percentage of net radiation (Engman and Gurney 1991).

Alternative Model Structures

The model structure employed herein and described in more detail previously (Croley and He 2005) applies the LBRM to each individual cell in the distributed approach. All subsurface flows (interflow and groundwater flow) enter the surface flow before the surface flow leaves the cell. This approach implies no subsurface flows between cells. The advantage of this approach is that it is relatively simple, computationally efficient, and easier to calibrate than approaches that allow subsurface flows. However, it is a very restrictive assumption and probably is the reason for the relatively poorer calibration statistics of the distributed-parameter LBRM compared with the lumped-parameter LBRM. We anticipate that the distributed-parameter LBRM calibration can be greatly improved by modifying the model to allow subsurface flows between cells. Each watershed cell is divided into an upper soil zone, a lower soil zone, and a groundwater zone (Croley and He 2005). Each successively flows into the next, and all flow into the surface storage of the cell's channel system.

As a first extension of the model structure, we would change the model to first allow an additional linear-reservoir flow out of the groundwater-zone storage into a downstream cell groundwater-zone storage; doing so would add an additional parameter to the model and change the continuity equations underlying the model (Croley and He 2005). We would then further modify the model to allow an additional flow into the groundwater-zone storage from the upstream cell. Thus, we would route the groundwater flows in a matter analogous to the surface routing. Most likely, we would employ the same drainage cascade of cells used for the surface routing; doing so implies that the groundwater divides of the watershed underlie the surface divides. These modifications would allow groundwater flow in each cell to the surface of that cell while also allowing groundwater contributions to continue in storage (other cell groundwater storages) before appearing at the outlet of the watershed. The

model structure changes and programming modifications would be similar to those already made to convert the lumped-parameter LBRM into the distributed-parameter version (Croley and He 2005).

As a second extension of the model structure, we would change the model similarly to route additional flows through the lower soil-zone storages of the watershed cells. That is, we allow an additional linear reservoir flow out of the lower soil-zone storage into a downstream cell lower soil-zone storage, thereby adding an additional parameter to the model. We would also allow an additional flow into the lower soil-zone storage from the upstream cell and route lower soil-zone flows (interflows) in a matter analogous to the surface and groundwater routings, again employing the same drainage cascade of cells determined by the surface topography. A third extension, if deemed worthwhile, would extend the distributed-parameter LBRM in an analogous fashion for the upper soil-zone storages in the watershed cells. The additional parameters would be considered spatially variable, as in Eqs. (3)–(7) or Eqs. (8)–(12).

These subsurface routing approaches should allow better consideration of landscape heterogeneity on subsurface hydrologic response than do the current distributed-parameter and lumped-parameter LBRM. They should also permit detailed accounting of the distribution of surface runoff, interflow, and groundwater throughout the watershed. The main challenge is calibrating additional interflow and groundwater parameters, since virtually no observed interflow and groundwater data are available over large areas in the Great Lakes basin. However, changing from 9 to 12 parameters is allowable with the degrees of freedom represented by the available data sets.

Summary

We adapted the large basin runoff model from its lumped-parameter formulation to a distributed-parameter formulation appropriate to model spatial watershed characteristics in the companion paper (Croley and He 2005) and applied it here to the Kalamazoo River watershed in southwest Michigan. We divided the watershed into a grid of 1-km^2 cells and assembled data for each cell on elevation, slope, land cover, flow roughness, upper soil-zone depth, upper soil permeability, lower soil-zone depth, and lower soil permeability. We used the data to estimate the spatial variability of model parameters as we calibrated the (spatial) mean values by matching observed Kalamazoo River flows.

The best-fit distributed-parameter model uses independent evapotranspiration and potential evapotranspiration (as opposed to complementary), which is appropriate for considering small-scale processes. It also uses a linear surface storage coefficient proportional to the square root of cell slope and inversely proportional to Manning's roughness. Upper soil-zone percolation to the lower soil zone and lower soil-zone interflow to the surface are described with linear reservoir coefficients proportional to upper soil permeability. Lower soil-zone deep percolation to the groundwater zone and groundwater flow to the surface are described with linear reservoir coefficients proportional to lower soil-zone permeability. Distributed-parameter model calibrations yield higher root-mean-square errors between observed and modeled Kalamazoo River flows than do lumped-parameter model applications. However, inspection of hydrographs reveals that the distributed-parameter model did a better job than the lumped-parameter model in matching variations in hydrograph recessions.

Solar insolation interpretation experiments showed that the best results come from using daily solar insolation derived from climate indices, as was done in the lumped-parameter model, in the absence of solar insolation observations. Calibration of a model that uses an hourly time interval yields no improvement over one that uses a daily time interval, probably because meteorology data were not available and diurnal modeling concepts were not utilized. However, the daily-hourly model comparisons yield similar results, suggesting that the daily time interval is small enough to allow the assumptions of constant precipitation, potential evapotranspiration, and upstream surface flow during each time interval. Several model extensions appear logical and include spatial routing of groundwater, interflow, or upper soil-zone flows.

Acknowledgments

Partial support for Chansheng He came from the National Research Council Research Associateship Program, and Western Michigan University Department of Geography Lucia Harrison Endowment Fund is acknowledged while he was on his sabbatical leave from GLERL.

References

Abdulla, F. A., Lettenmaier, D. P., Wood, E. F., and Smith, J. A. (1996). "Application of a macroscale hydrologic model to estimate the water balance of the Arkansas–Red River Basin." *J. Geophys. Res.*, 101(D3), 7449–7459.

Beasley, D. B., Huggins, L. F., and Monke, E. J. (1980). "ANSWERS: A model for watershed planning." *Trans. ASAE*, 23(4), 938–944.

Becker, A., and Braun, P. (1999). "Disaggregation, aggregation and spatial scaling in hydrological modeling." *J. Hydrol.*, 217, 239–252.

Beven, K. J. (2000). *Rainfall-runoff modeling: The primer*, Wiley, New York.

Bicknell, B. R., Imhoff, J. C., Kittle, J., Donigian, A. S., and Johansen, R. C. (1996). *Hydrological simulation program—FORTRAN, user's manual for release 11*, U.S. Environmental Protection Agency, Environmental Research Laboratory, Athens, Ga.

Caselles, V., Artigao, M. M., Hurtado, E., Coll, C., and Brasa, A. (1998). "Mapping actual evapotranspiration by combing Landsat TM and NOAA-AVHRR images: Application to the Barrax area, Albacete, Spain." *Remote Sens. Environ.*, 63, 1–10.

Cosby, B. J., Hornberger, G. M., Clapp, R. B., and Ginn, T. R. (1984). "A statistical exploration of the relationships of soil moisture characteristics to the physical properties of soils." *Water Resour. Res.*, 20(6), 682–690.

Crawford, N. H., and Linsley, R. K. (1966). "Digital simulation in hydrology: Stanford Watershed Model IV." *Technical Report39*, Dept. of Civil Engineering, Stanford Univ., Calif.

Croley, T. E., II. (2002). "Large basin runoff model." *Mathematical models in watershed hydrology*, V. Singh, D. Frevert, and S. Meyer, eds., Water Resources Publications, Littleton, Colo., 717–770.

Croley, T. E., II, and He, C. (2005). "Distributed-parameter large basin runoff model. I: Model development." *J. Hydrologic Eng.*, 10(3), .

Dingman, S. L (2002). *Physical hydrology*, 2nd Ed., Prentice Hall, Upper Saddle River, N.J., 428.

Engman, E. T., and Gurney, R. J. (1991). *Remote sensing in hydrology*, Chapman and Hall, New York.

Goodrich, D. C., Lane, L. J., Shillito, R. M., Miller, S. N., Syed, K. H., and Woolhiser, D. A. (1997). "Linearity of basin response as a function of scale in a semiarid watershed." *Water Resour. Res.*, 33(12), 2951–2965.

He, C., Shi, C., Yang, C., and Agosti, B. P. (2001). "A Windows-based

GIS-AGNPS interface." *J. Am. Water Resour. Assoc.*, 37(2), 395–406.
Jensen, M. E., Burman, R. D., and Allen, R. G. (1990). "Evapotranspiration and irrigation water requirement." *ASCE Manuals and Reports on Engineering Practice No. 70*, New York.
Karvonen, T., Koivusalo, H., Jauhiainen, M., Palko, J., and Weppling, K. (1999). "A hydrological model for predicting runoff from different land use areas." *J. Hydrol.*, 217, 253–265.
Leavesley, G. H., and Stannard, L. G. (1995). "The precipitation-runoff modeling system—PRMS." *Computer models of watershed hydrology*, V. P. Singh, ed., Water Resource Publications, Highlands Ranch, Colo., 281–310.
Liang, X., Lettenmaier, D. P., Wood, E. F., and Burges, S. J. (1994). "A simple hydrologically based model of land surface water and energy fluxes for generation circulation models." *J. Geophys. Res.*, 99(D7), 14415–14428.
Mays, L. W. (2001). *Water resources engineering*, Wiley, New York, 92.
Richardson, C. W., and Wright, D. A. (1984). "WGEN: A model for generating daily weather variables." *ARS-8*, U.S. Dept. of Agriculture, Agricultural Research Service.
USDA Soil Conservation Service (USDA SCS). (1993). "State Soil Geographic Data Base (STATSGO)." *Miscellaneous Publication No. 1492*, U.S. Government Printing Office, Washington, D.C.
Wood, E. G., and Lakshmi, V. A. (1993). "Scaling water and energy fluxes in climate systems: Three land-atmospheric modeling experiments." *J. Clim.*, 6, 839–857.
Xu, C.-Y., and Singh, V. P. (1998). "Dependence of evaporation on meteorological variables at different time-scales and intercomparison of estimation methods." *Hydrolog. Process.*, 12, 429–442.
Yu, Z., Carlson, T. N., Barron, E. J., and Schwartz, F. W. (2001). "On evaluating the spatial variation of soil moisture in the Susquehanna River Basin." *Water Resour. Res.*, 37(5), 1313–1326.